Clin Orthop Relat Res (2018) 476:1665-1679
DOI 10.1097/CORR.0000000000000335

Clinical Orthopaedics and Related Research®
A Publication of The Association of Bone and Joint Surgeons®

Basic Research

Reversal of Fatty Infiltration After Suprascapular Nerve Compression Release Is Dependent on UCP1 Expression in Mice

Zili Wang MD, Brian T. Feeley MD, Hubert T. Kim MD, PhD, Xuhui Liu MD

Received: 31 October 2017 / Accepted: 12 April 2018 / Published online: 17 July 2018

Abstract

Background In large rotator cuff tears, retraction of the supraspinatus muscle creates suprascapular nerve traction and compression. However, suprascapular nerve transection, when used in previous models, is different from chronic compression of the suprascapular nerve in patients. To define the role of suprascapular nerve chronic injury in rotator cuff muscle atrophy and fatty infiltration, we developed a novel reversible suprascapular nerve compression mouse model.

Questions/purposes We asked: (1) Can suprascapular nerve injury be induced by compression but reversed after compression release? (2) Can muscle fatty infiltration be induced by suprascapular nerve compression and reversed after compression release? (3) Is white fat browning involved in fatty infiltration resorption?

Methods Mice in a common strain of C57BL/6J were randomly assigned to suprascapular nerve transection (n = 10), nerve compression (n = 10), nerve compression and release (n = 10), or sham control (n = 10) groups. To study the role or white fat browning on muscle fatty infiltration, additional UCP1 reporter mice (n = 4 for nerve compression and n = 4 for nerve compression release) and knockout mice (n = 4 for nerve compression and n = 4 for nerve compression release) were used. Nerve injury was testified using osmium tetroxide staining and neural muscular junction staining and then semiquantified by counting the degenerating axons and disrupted junctions. Muscle fatty infiltration was evaluated using Oil Red O staining and then semiquantified by measuring the area fraction of fat. Immunofluorescent and Oil Red O staining on UCP1 transgenic mice was conducted to testify whether white fat browning was involved in fatty infiltration resorption. Ratios of UCP1 positively stained area and fat area to muscle cross-section area were measured to semiquantify UCP1 expression and fatty infiltration in muscle by blinded reviewers. Analysis of variance with Tukey post hoc comparisons was used for statistical analysis between groups.

The institution of one of the authors (ZW; Third Xiangya Hospital of Central South University) received, during the study period, a training fund in the amount of USD 20,400 per year from the China Scholarship Council to support studying at the University of California, San Francisco. The institution of the authors (ZW, BTF, HTK, XL; San Francisco Veterans Affairs Medical Center) received, during the study period, funding from the VA BLR&D Merit review grant (HTK; 1 I01 BX002680-01A2) in the amount of USD 150,000 per year. The institution of the authors (ZW, BTF, HTK, XL; University of California at San Francisco) received, during the study period, funding from the UCSF Core Center for Musculoskeletal Biology and Medicine (BTF; National Institutes of Health 1P30AR066262-01) in the amount of USD 40,000 per year.
Clinical Orthopaedics and Related Research® neither advocates nor endorses the use of any treatment, drug, or device. Readers are encouraged to always seek additional information, including FDA approval status, of any drug or device before clinical use.
Each author certifies that his institution approved the animal protocol for this investigation and that all investigations were conducted in conformity with ethical principles of research.
This work was performed at the San Francisco Veterans Affair Health Medical Center, San Francisco, CA, USA.

Z. Wang, Department of Orthopaedic Surgery, Third Xiangya Hospital of Central South University, Changsha, Hunan Province, China

Z. Wang, B. T. Feeley, H. T. Kim, X. Liu, San Francisco Veterans Affairs Medical Center, Department of Veterans Affairs, San Francisco, CA, USA; and the Department of Orthopedic Surgery, University of California at San Francisco, San Francisco, CA, USA

X. Liu (✉), San Francisco Veterans Affairs Medical Center, Department of Veterans Affairs, 1700 Owens Street, San Francisco, CA 94158, USA, email: liu.xuhui@ucsf.edu

All ICMJE Conflict of Interest Forms for authors and *Clinical Orthopaedics and Related Research*® editors and board members are on file with the publication and can be viewed on request.

Wolters Kluwer

Results Suprascapular nerve injury was induced by compression but reversed after release. The ratios of degenerating axons were: sham control: 6% ± 3% (95% confidence interval [CI], 3%-10%); nerve compression: 58% ± 10% (95% CI, 45%-70% versus sham, $p < 0.001$); and nerve compression and release: 15% ± 9% (95% CI, 5%-26% versus sham, $p = 0.050$). The supraspinatus muscle percentage area of fatty infiltration increased after 6 weeks of nerve compression (19% ± 1%; 95% CI, 18%-20%; $p < 0.001$) but showed no difference after compression release for 6 weeks (5% ± 3%; 95% CI, 1%-10%; $p = 0.054$) compared with sham (2% ± 1%; 95% CI, 1%-3%). However, the fat area fraction in UCP1 knockout mice did not change after nerve compression release (6% ± 1%; 95% CI, 4%-8% at 2 weeks after compression and 5% ± 0.32%; 95% CI, 4%-6% after 2 weeks of release; $p = 0.1095$).
Conclusions We developed a clinically relevant, reversible suprascapular nerve compression mouse model. Fatty infiltration resorption after compression release was mediated through white fat browning.
Clinical Relevance If the mechanism of browning of white fat in rotator cuff muscle fatty infiltration can be confirmed in humans, a UCP1 agonist may be an effective treatment for patients with suprascapular nerve injury.

Introduction

Rotator cuff tears are the most common tendon injury in the adult population, affecting at least 10% of people older than 60 years of age in the United States [13]. Accumulating evidence suggests that suprascapular nerve entrapment and traction after large or massive rotator cuff tears are involved in supraspinatus and infraspinatus muscle atrophy and fatty infiltration, which are important factors responsible for failed tendon repairs [5, 27, 35]. Thus, defining the role of suprascapular nerve neuropathy in supraspinatus and infraspinatus muscle atrophy and fatty infiltration is critical to understanding the mechanisms of secondary muscle degeneration after rotator cuff tears and the development of a treatment strategy to improve rotator cuff muscle function after rotator cuff repair. Currently, it is rare for interventions to be performed on the suprascapular nerve at the time of rotator cuff repair, and understanding how the nerve directly reacts to traction and compression may change clinical practice or improve muscle quality (and perhaps clinical outcomes) after rotator cuff repair.

We have previously developed rodent models of massive rotator cuff tears with transection of the suprascapular nerve to study the mechanisms of muscle atrophy and fatty infiltration with suprascapular nerve injury [30, 31]. In those models, we observed muscle atrophy and fatty infiltration after suprascapular nerve transection, suggesting a critical role of suprascapular nerve neuropathy involved in muscle pathology after massive rotator cuff tears. We subsequently found that suprascapular nerve transection and rotator cuff transection use different pathways in rotator cuff muscle degeneration [20]. Our models were well accepted by the field and have been used by multiple groups in their studies [2, 16, 26, 38]. However, those models are limited by the fact that the acute transection does not completely simulate chronic compression of the suprascapular nerve injury seen in patients with rotator cuff tears.

In humans and many other vertebrate animals including mice, there are two types of fat with distinct phenotypes and functions: white fat to store energy and brown fat to generate heat. Recent studies have discovered some white fat-like fat is actually an interchangeable form, named beige or brite fat, which can become brown-like fat in response to appropriate stimuli [22, 23, 28, 29]. This process, termed "white fat browning," is mediated by uncoupling protein 1 (UCP1) to dissipate energy. "Browning of white fat" has becoming a potential therapeutic intervention to treat obesity and metabolic diseases in recent years [18, 24]. However, it remains unknown if brown or beige fat is involved in muscle fatty infiltration.

In this study, we hypothesized that isolation and ligation of the suprascapular nerve would result in marked muscle atrophy and fatty infiltration and that release of the nerve would result in muscle quality improvement as measured by functional outcomes (gait analysis) and histologic analysis. We further suggested that beige fat, as determined by UCP1 expression, would be a key factor in the ability of the muscle to decrease fat after nerve release. We developed a novel mouse model of chronic suprascapular nerve compression.

Specifically, using that model, we asked: (1) Can suprascapular nerve injury be induced by compression but reversed after compression release? (2) Can fatty infiltration of muscle be induced by suprascapular nerve compression and reversed after compression release? (3) Is white fat browning involved in fatty infiltration resorption?

Materials and Methods

Experimental Overview

Eight-week-old adult mice were used in this study. These included 45 female C57BL/6J mice (Jackson Laboratory Inc, Sacramento, CA, USA, stock # 000664), eight UCP1 reporter male mice (FVB/N-Tg[Ucp1-luc2,-tdTomato] 1Kajim/J, JAX stock # 026690), and eight UCP1-KO female mice (129S-Ucp1^{tm1Kz}/J, JAX stock # 017476) that Dr Shingo Kajimura of the University of California at San Francisco provided as gifts. Only female C57B/L6J mice were used in the present study, because no sex differences were found in a pilot study. In UCP1 reporter mice, the UCP1 reporter gene was inserted into the Y chromosome.

Thus, only male UCP1 reporter mice were used. Both male and female UCP1 knockout mice were used in this study. Mice were randomized into sham and experimental groups. According to our preliminary experiment, power analysis was performed using an estimated 15% difference in area fraction of fat in muscle between the sham group and the nerve compression group. With $\beta = 0.80$ and $\alpha = 0.05$, we determined that four mice per group would be sufficient to demonstrate a difference of 18% in muscle fat area fraction between the sham and nerve compression groups, which is the effect size we considered clinically important. For the C57BL/6J mice, 10 animals underwent unilateral suprascapular nerve transection to establish denervation of the supraspinatus and infraspinatus (five mice for histologic staining and five mice for quantitative polymerase chain reaction analysis, 10 mice underwent unilateral suprascapular nerve compression surgery, 10 mice underwent unilateral suprascapular nerve compression for 6 weeks and then release, 10 mice underwent unilateral sham surgery, and five mice served as baseline controls for gait analysis). For UCP1 reporter mice, four UCP1 (-/-) (knockout) and four UCP1 (+/+) (wild-type control for UCP1 KO) mice underwent unilateral suprascapular nerve compression for 2 weeks. Another four UCP1 (-/-) and four UCP1 (+/+) mice underwent unilateral suprascapular nerve compression for 2 weeks and then release (Fig. 1).

Conditions and diet were identical for all animals. Mice were housed and cared for in accordance with the New Zealand Animal Welfare Act [34]. All procedures were approved by our institutional animal care and use committee.

The primary outcome was the fatty infiltration in supraspinatus and infraspinatus muscles. Secondary outcomes were the UCP1 expression in supraspinatus and infraspinatus muscles, nerve regeneration, wet muscle weight, gene expression, gait analysis, and muscle fibrosis.

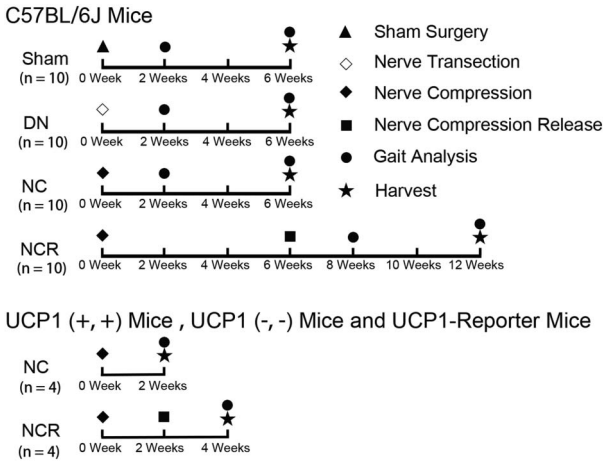

Fig. 1 The flow diagram exhibits our experiment design. DN = denervation; NC = nerve compression; NCR = nerve compression and release.

Surgical Procedures

For the suprascapular nerve transection surgery, after general anesthesia by 3% isoflurane, the right-sided suprascapular nerve was transected as described previously [30]. For the suprascapular nerve compression and release, after the skin incision, the trapezius muscle was separated to expose the suprascapular nerve. After it was identified, the suprascapular nerve was wrapped in a sterile 1 mm x 1 mm x 50-mm polyethylene sheet to form a tube (Fisher Scientific™, Waltham, MA, USA) at the site immediately after it was derived from the superior trunk of the bronchial plexus. The tube was ligated at each end with 7-0 nylon sutures. The sutures and polyethylene tube were removed at 2 weeks or 6 weeks after compression in some animals (Fig. 2). The trapezius muscles and skin were closed at both suprascapular nerve compression and release procedures. For the sham surgery, the skin and muscle incisions were performed, the suprascapular nerve was identified, and the muscle and skin were then closed.

Gait Analysis

DigiGait™ (Mouse Specifics Inc, Quincy, MA, USA) analysis was conducted to measure shoulder function at the day of harvest as described previously [6]. All animals were weighed to confirm that there were no statistical differences among all groups before being euthanized (data not shown). All mice walked 10 cm/s for 10 seconds on the DigiGait system. Stride length, stance width, and paw area at peak stance were chosen for the parameters to assess forelimb function [9, 25].

Sample Harvesting, Wet Muscle Weight, and Histology

After the mice were euthanized, we harvested the bilateral supraspinatus (SS) and infraspinatus (IS) muscles. For assessing muscle atrophy, we measured the wet weight of bilateral supraspinatus and infraspinatus muscles immediately after harvesting. The percent change of wet muscle weight was measured using the following equation: $([SS_{Right} - SS_{Left}]/SS_{Left}) \times 100\%$ or $([IS_{Righ\ t} - IS_{Left}]/IS_{Left}) \times 100\%$ 12. After weighing, the supraspinatus and infraspinatus muscles were mounted on cork disks (Fisher Scientific) with 10% w/v tragacanth gum (Sigma-Aldrich, St Louis, MO, USA) and flash frozen in liquid nitrogen-cooled 2-methylbutane followed by a 10-μm cryosection for muscle histology staining or 20-μm cryosection for neuromuscular junction staining. Masson trichrome (American MasterTech, Lodi, CA, USA) and Oil Red O (Sigma-Aldrich) staining were conducted to assess the fibrosis and fatty infiltration in the muscle.

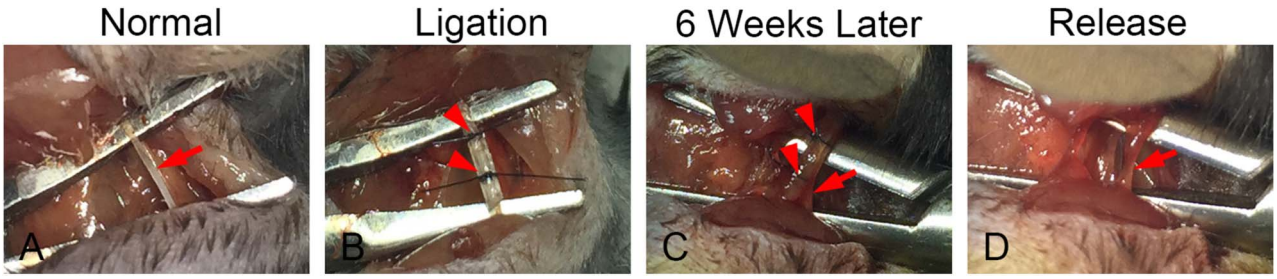

Fig. 2 A-D Surgery of suprascapular nerve compression and release is shown. (**A**) After the trapezius muscle was separated, the suprascapular nerve was exposed. (**B**) The suprascapular nerve was wrapped by a 1 mm x 1 mm x 5-mm polyethylene sheet at the site, which was then ligated by 7-0 nylon sutures at each end. (**C**) Six weeks later, the suprascapular nerve, the polyethylene sheet, and sutures were exposed. (**D**) The polyethylene sheet and sutures were removed and the suprascapular nerve was released. Arrows indicate suprascapular nerve and arrowheads indicate sutures and polyethylene sheets.

A segment of the suprascapular nerve distal to the compression site was also harvested to evaluate the nerve injury and recovery after compression/release. After fixing using 4% paraformaldehyde (Fisher Scientific) overnight, the suprascapular nerve was stained with 2% osmium tetroxide (Sigma-Aldrich) for 120 minutes, dehydrated in grading ethanol and xylene, embedded in paraffin, and then divided into 7-mm sections as previously described [19].

Immunofluorescence Staining

Neuromuscular junction staining for C57BL/6J mice was performed as previously described [4]. Samples were fixed in 4% paraformaldehyde for 30 minutes, rinsed in phosphate-buffered saline (PBS) for 10 minutes three times, placed in 0.1 M glycine (Fisher Scientific, diluted in PBS) for 30 minutes, and washed again for 3 x 10 minutes in PBS. They were then immersed in 100% methanol for 5 minutes at -20° C, rinsed for 3 x 10 minutes in PBS, and covered with blocking solution (0.2% Triton X-100, 2% bovine serum albumin in PBS) for 1 hour at room temperature. Primary antibodies (Developmental Studies Hybridoma Bank, Iowa City, IA, USA) against neurofilament (NF-2H3, diluted 1:250) and synaptic vesicle protein 2 (SV2, diluted 1:250) were diluted in a block mix and added to the sections for overnight incubation at 4° C. The next day, samples were rinsed in PBS for 3 x 10 minutes and incubated in a mixture containing rhodamine conjugated alpha-bungarotoxin (T0195, Sigma-Aldrich, diluted 1:200) and FITC-conjugated donkey anti-mouse IgG (ab150109, Abcam, Burlingame, CA, USA; diluted 1:250) at room temperature for 120 minutes. Sections were then rinsed for 20 minutes in PBS and mounted with coverslips using VectaShield with DAPI (H-1200; Vector Laboratories, Burlingame, CA, USA).

For UCP1 reporter mice, sections were fixed in 4% paraformaldehyde for 30 minutes, rinsed in PBS for 30 minutes, incubated with blocking solution (the same as previously described) for 60 minutes, and subsequently treated with the primary antibody (anti-Laminin, L9393, Sigma-Aldrich, 1:500 diluted in blocking solution) at 4° C overnight. After a PBS rinse for 3 x 10 minutes, the sections were incubated with secondary antibody (ab150073, Alexa Fluor 488- and conjugated antirabbit IgG) for 120 minutes. After a PBS rinse for 2 x 10 minutes, the slides were mounted with coverslips using VectaShield with DAPI.

Image Capture and Quantification

Histology images were observed on an optical microscope (Axio Imager; Zeiss, Oberkochen, Germany), and fluorescent images were acquired using an Axio Observer D1 fluorescence microscope. Pictures were analyzed using image analysis software (ImageJ; National Institutes of Health, Bethesda, MD, USA). All pictures were assessed by two blinded reviewers (ZW, KJ). For osmium staining, an average of 700 axons per group was evaluated, and the ratio of axons with abnormal myelin (myelin reduplication, splitting of the myelin sheath, and detachment of the myelin sheath from the axon) was calculated by dividing the number of abnormal axons by the number of entire axons [3]. For neuromuscular junction staining, we evaluated 212 to 230 neuromuscular junctions per group. We calculated the ratio of disrupted neuromuscular junctions (acetylcholine receptor with absence of neurofilament) by dividing the number of disrupted neuromuscular junctions by the number of total neuromuscular junctions [4]. Cross-section area was measured with muscle fibers in five randomly selected areas on sections from the midbelly of the supraspinatus and infraspinatus muscles. The area fraction of fibrosis was calculated by dividing the area of Aniline Blue staining collagenous fibrotic area by the entire sample area. Similarly, the area fraction of fatty infiltration was assessed by dividing the area of Oil Red O staining fat area by the entire sample area [30, 31]. To evaluate UCP1

expression in muscle, we calculated the ratio of UCP1 area by dividing the UCP1 stained area by the entire sample area.

Reverse Transcription-Polymerase Chain Reaction

Total RNA for the supraspinatus/infraspinatus pooled muscle samples was extracted using Trizol reagent (Fisher Scientific) according to the instructions. The Transcriptor First Strand cDNA Synthesis Kit (Roche Applied Bioscience Inc, Indianapolis, IN, USA) was applied to synthesize cDNA. We performed reverse transcription-polymerase chain reaction (RT-PCR) to quantify the expression of Atroin-1, Murf-1, a-SMA, collagen-1a, collagen-3a, PPAR-γ1, PPAR-γ2, C/EBP-a, and Adipoq using SYBR Green Detection and an Applied Biosystems Prism 7900HT detection system (Applied Biosystems Inc, Foster City, CA, USA). Sequences of the primers for target genes were summarized (Table 1). The expression level of each gene was normalized to that of the housekeeping gene of S26. Fold changes relative to sham controls were calculated using ΔΔCT.

No animal died; no skin wound infections or other unexpected adverse events were observed in this study.

Statistical Analysis

Analyses of variance with Tukey post hoc comparisons were used to calculate the difference in the ratio of degenerating axons, ratio of injured neuromuscular junction, percent wet muscle weight change, area fraction of collagen, area fraction of fat, gene expression, gait analysis, and ratio of UCP1 area among all groups. For the 6-week nerve compression and release group, Pearson correlation coefficient was used to evaluate the correlation between the gait analysis and the fat area fraction in muscle. All data are presented as mean ± SD. Statistical significance was set at $p < 0.05$.

Results

Suprascapular Nerve Injury Was Induced by Compression and Reversed After Compression Release

The denervation group and the nerve compression group demonstrated more degenerating axons than the sham group. We observed 78% ± 18% (mean ± SD) (95% confidence interval [CI], 55%-100%; $p < 0.001$ compared with sham) of degenerating axons in the denervation group and 58% ± 10% (95% CI, 45%-70%; $p < 0.001$ compared with sham) in the nerve compression group. However, for the nerve compression and release group, we only found 15% ± 9% (95% CI, 5%-26%) of axons with abnormal myelin, which was lower than the nerve compression group ($p < 0.001$). However, no difference was found when comparing the compression and release group with the sham group ($p = 0.050$; Fig. 3A-D).

Compared with the sham group (ratio of disrupted neuromuscular junctions in the supraspinatus: 1% ± 0.18%, 95% CI, 1%-2%; in the infraspinatus: 1% ± 0.25%, 95% CI, 0.81%-1.42%), we found greater neuromuscular junction disruption (acetylcholine receptors with absence of neurofilament) in the denervation group (ratio of disrupted neuromuscular junctions in the supraspinatus: 93% ± 7%, 95% CI, 85%-102%, $p < 0.001$; in the infraspinatus: 87% ± 9%, 95% CI, 77%-98%, $p < 0.001$) and the nerve compression group (ratio of disrupted neuromuscular junctions in the supraspinatus: 71% ± 21%, 95% CI, 45%-97%, $p < 0.001$; in the infraspinatus: 65% ± 20%, 95% CI, 41%-90%, $p < 0.001$). However, we observed substantial neuromuscular junction recovery in the nerve compression and release group. No difference was found with the disrupted neuromuscular junctions between the sham group and the nerve compression and release group (ratio of disrupted neuromuscular junctions in the supraspinatus: 8% ± 7%, 95% CI, -0.12% to 16%, $p = 0.052$; in the infraspinatus: 11% ± 9%, 95% CI, 1%-22%, $p = 0.0537$) (Fig. 3E-L).

Table 1. Sequence of murine gene primers

Gene	Forward primer sequence (5′→3′)	Reverse primer sequence (5′→3′)
Atrogin-1	CCATCAGGAGAAGTGGATCTATGTT	GCTTCCCCCAAAGTGCAGTA
Murf-1	TGTTCTGGTAGGTCGTTTCCG	ATGCCGGTCCATGATCACTT
a-SMA	GGACGTACAACTGGTATTGTGC	TCGGCAGTAGTCACGAAGGA
Collagen 1a	GCTCCTCTTAGGGGCCACT	ATTGGGGACCCTTAGGCCAT
Collagen 3a	CAGGACCTAAGGGCGAAGATG	TCCGGGCATACCCCGTATC
PPAR-g1	TCGCTGATGCACTGCCTATG	GAGAGGTCCACAGAGCTGATT
PPAR-g2	GGAAGACCACTCGCATTCCTT	GTAATCAGCAACCATTGGGTCA
c/EBP-a	GCGGGAACGCAACAACATC	GTCACTGGTCAACTCCAGCAC
Adipoq	GTTCCCAATGTACCCATTCGC	TGTTGCAGTAGAACTTGCCAG
s26	TCATTCGGAACATTGTAGAAGCC	AGCTTGACATAGAGCTTGGGAA

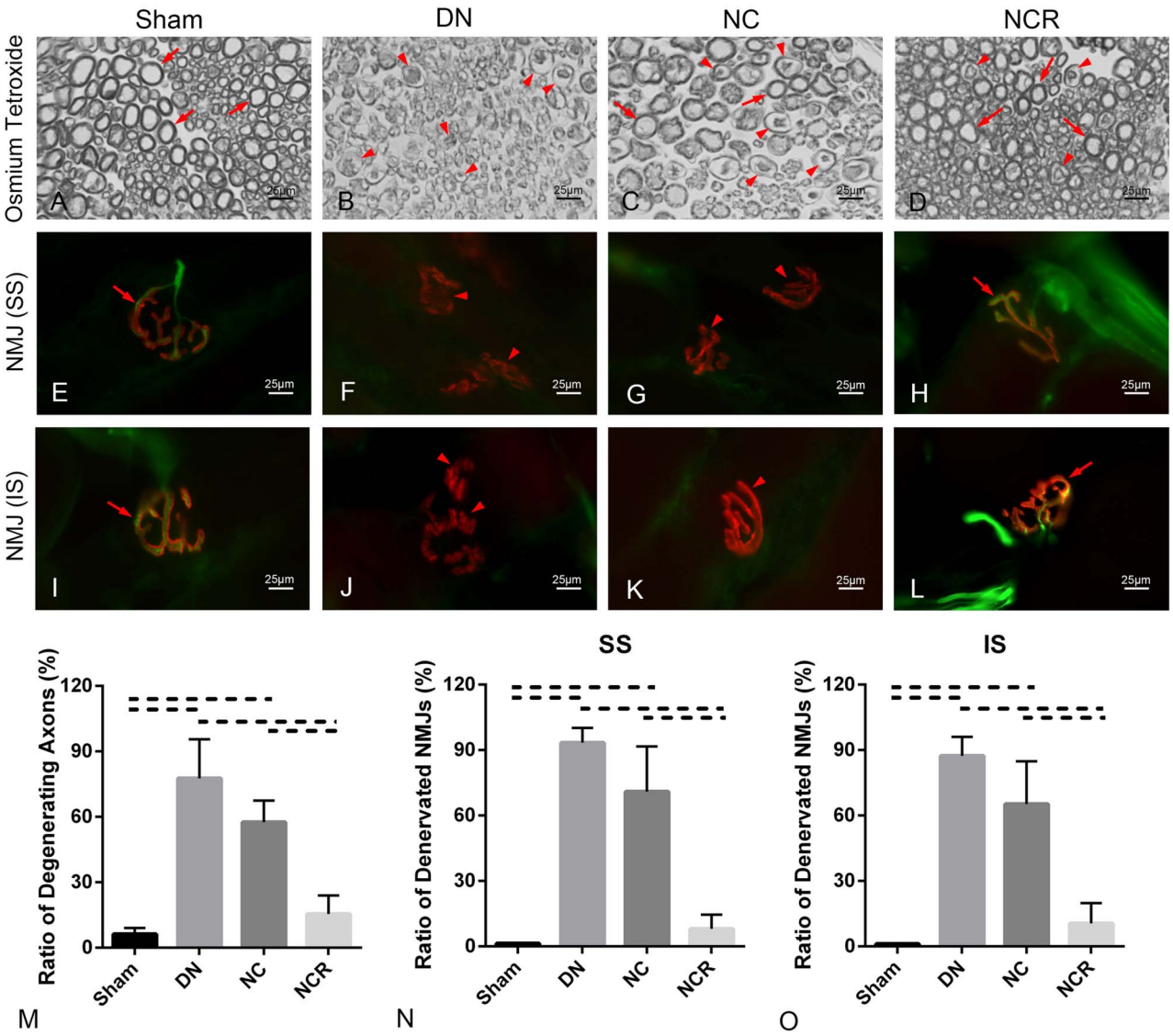

Fig. 3 A-O (**A-D**) Micrographs of suprascapular nerve cross-sections were stained with 2% osmium tetroxide (original magnification, x 1000). Arrows indicate normal axon, and arrowheads indicate degenerating axons. (**E-L**) Neuromuscular junction staining of supraspinatus and infraspinatus is shown (original magnification, x 1000); acetylcholine receptors are red, axons green; arrows indicate normal or reinnervated neuromuscular junction and arrowheads indicate denervated neuromuscular junction. (**M**) Ratio of degenerating axon in suprascapular nerve (%) = degenerating axons/entire axons. (**N-O**) Ratio of the denervated neuromuscular junction in both supraspinatus and infraspinatus (%) = number of denervated neuromuscular junction/number of entire neuromuscular junction; solid lines indicate $p < 0.05$, and dashed lines indicate $p < 0.01$. Error bars indicate SD. DN = denervation; NC = nerve compression; NCR = nerve compression and release; NMJ = neuromuscular junction; SS = supraspinatus; IS = infraspinatus.

Muscle Fatty Infiltration Was Induced by Suprascapular Nerve Compression but Reversed After Compression Release

The denervation, nerve compression, and nerve compression and release groups had more muscle weight loss percentage and smaller muscle fiber cross-sectional area when compared with the sham group (for supraspinatus muscle weight loss percentage, the sham group: -2% ± 1%, 95% CI, -3% to -0.2%; the denervation group: -48% ± 7%, 95% CI, -56% to -39%, $p < 0.001$; the nerve compression group: -41% ± 8%, 95% CI, -50% to -32%, $p < 0.001$; the nerve compression and release group: -20% ± 7%, 95% CI, -28% to -11%, $p < 0.001$; for infraspinatus muscle weight loss percentage, the sham group: -1% ± 1%, 95% CI, -3% to -0.12%; the denervation group: -46% ± 6%, 95% CI, -53% to -38%, $p < 0.001$; the nerve compression group: -41% ± 5%, 95% CI, -47% to -36%, $p < 0.001$; the nerve

compression and release group: -16% ± 10%, 95% CI, -29% to -4%, p = 0.012; for supraspinatus muscle fiber cross-sectional area, the sham group: 1972 ± 342 μm^2, 95% CI, 1547-2397 μm^2; the denervation group: 968 ± 258 μm^2, 95% CI, 647-1289 μm^2, p < 0.001 compared with sham; the nerve compression group: 1201 ± 322 μm^2, 95% CI, 802-1601 μm^2, p = 0.006 compared with sham; the nerve compression and release group: 1659 ± 127 μm^2, 95% CI, 1502-1817 μm^2, p = 0.1268 compared with sham; for infraspinatus muscle fiber cross-sectional area, the sham group: 1686 ± 306 μm^2, 95% CI, 1307-2066 μm^2; the denervation group: 801 ± 119 μm^2, 95% CI, 653-948 μm^2, p < 0.001 compared with sham; the nerve compression group: 1092 ± 266 μm^2, 95% CI, 761-1423 μm^2, p = 0.011 compared with sham; the nerve compression and release group: 1475 ± 155 μm^2, 95% CI, 1283-1667 μm^2, p = 0.205 compared with sham). However, we found that the compression and release group demonstrated less muscle weight loss percentage and bigger muscle fiber cross-sectional area than the nerve compression group (supraspinatus muscle weight loss percentage, p = 0.001, infraspinatus, p = 0.001; supraspinatus muscle fiber cross-sectional area, p = 0.0098, infraspinatus, p = 0.0239) (Fig. 4).

Compared with the sham group (collagen area fraction in supraspinatus: 4% ± 2%, 95% CI, 2%-6%; collagen area fraction in infraspinatus: 3% ± 2%, 95% CI, 1%-5%; fat area fraction in supraspinatus: 2% ± 1%, 95% CI, 1%-3%; fat area fraction in infraspinatus: 2% ± 1%, 95% CI, 1%-2%), we observed more fibrosis and fatty infiltration in the supraspinatus and infraspinatus muscles from the denervation group (collagen area fraction in supraspinatus: 32% ± 4%, 95% CI, 27%-36%, p < 0.001 compared with sham; collagen area fraction in

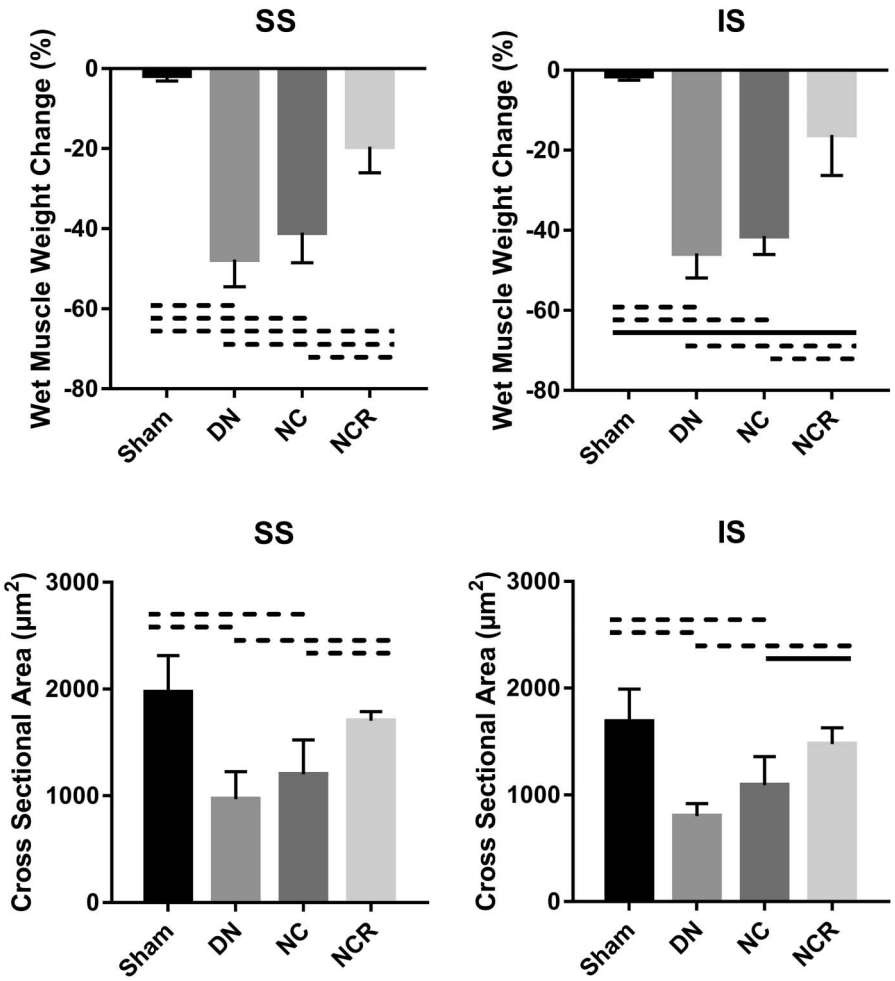

Fig. 4 Percent wet muscle weight change and muscle fiber cross-sectional area of the supraspinatus and infraspinatus are shown. Solid lines indicate p < 0.05, and dashed lines indicate p < 0.01. Error bars indicate SD. DN = denervation; NC = nerve compression; NCR = nerve compression and release; SS = supraspinatus; IS = infraspinatus.

infraspinatus: 33% ± 3%, 95% CI, 30%-37%, $p < 0.001$ compared with sham; fat area fraction in supraspinatus: 20% ± 2%, 95% CI, 17%-23%, $p < 0.001$ compared with sham; fat area fraction in infraspinatus: 19% ± 3%, 95% CI, 15%-22%, $p < 0.001$ compared with sham) and the nerve compression group (collagen area fraction in supraspinatus: 26% ± 5%, 95% CI, 20%-31%, $p < 0.001$ compared with sham; collagen area fraction in infraspinatus: 25% ± 8%, 95% CI, 15%-35%, $p < 0.001$ compared with sham; fat area fraction in supraspinatus: 19% ± 1%, 95% CI, 18%-20%, $p < 0.001$ compared with sham; fat area fraction in infraspinatus: 17% ± 2%, 95% CI, 14%-20%, $p < 0.001$ compared with sham). However, compared with the nerve compression group, fibrosis and fatty infiltration were reduced in the nerve compression and release group (collagen area fraction in supraspinatus: 7% ± 2%, 95% CI, 4%-10%, $p < 0.001$; collagen area fraction in infraspinatus: 6% ± 3%, 95% CI, 2%-9%, $p < 0.001$; fat area fraction in supraspinatus: 5% ± 3%, 95% CI, 1%-10%, $p < 0.001$; fat area fraction in infraspinatus: 5% ± 3%, 95% CI, 1%-8%, $p < 0.001$) (Fig. 5). Atrophy, fibrosis, and fatty infiltration-related gene expression were upregulated 3.5- to 4.5-fold in the denervation group and three- to fourfold in the nerve compression group. No major differences of atrophy, fibrosis, or fatty infiltration-related gene expression were found in the nerve compression and release group when compared with the sham group (Fig. 6).

Compared with the sham group (stride length: 3.06 ± 0.52 cm, 95% CI, 2.42-3.71 cm; stance width: 1.62 ± 0.16 cm, 95% CI, 1.42-1.82 cm; paw area at peak stance: 0.29 ± 0.06 cm^2, 95% CI, 0.22-0.37 cm^2), the injured limb function in the nerve compression and release group recovered 6 weeks after repair (stride length: 2.62 ± 0.12 cm, 95% CI, 2.47-2.76 cm, $p = 0.095$; stance width: 1.55 ± 0.12 cm, 95% CI, 1.40-1.70 cm, $p = 0.436$; paw area at peak stance: 0.26 ± 0.03 cm^2, 95% CI, 0.22-0.30 cm^2, $p = 0.2938$). However, the injured limb function in animals in the denervation and nerve compression groups remained inferior to the sham group at 6 weeks postoperatively (for the denervation group, stride length: 1.80 ± 0.52 cm, 95% CI, 1.15-2.45 cm, $p = 0.0048$; stance width: 1.18 ± 0.15 cm, 95% CI, 0.99-1.37 cm, $p = 0.002$; paw area at peak stance: 0.16 ± 0.04 cm^2, 95% CI, 0.11-0.21 cm^2, $p = 0.003$; for the nerve compression group, stride length: 2.11 ± 0.24 cm, 95% CI, 1.81-2.41 cm, $p = 0.0057$; stance width: 1.27 ± 0.08 cm, 95% CI, 1.17-1.37 cm, $p = 0.002$; paw area at peak stance: 0.19 ± 0.03 cm^2, 95% CI, 0.16-0.22 cm^2, $p = 0.007$) (Fig. 7). A correlation coefficient was applied to determine the correlation between the shoulder functional data (gait analysis) and the fat area fraction in the supraspinatus and infraspinatus muscles in the nerve compression and release group. For both the supraspinatus and infraspinatus muscles, fat area fraction showed a high correlation to stride length, stance width, and paw area at peak stance (for supraspinatus, r value of fat area fraction and stride length = -0.907, $p = 0.033$, r value of fat area fraction and stance width = -0.902, $p = 0.036$, r value of fat area fraction and paw area at peak stance = -0.983, $p = 0.003$; for infraspinatus, r value of fat area fraction and stride length = -0.950, $p = 0.013$, r value of fat area fraction and stance width = -0.912, $p = 0.031$, r value of fat area fraction and paw area at peak stance = -0.994, $p = 0.001$) (Table 2).

Muscle Fatty Infiltration After Suprascapular Nerve Compression and Release Is Related to Browning of White Fat

UCP1 expression was increased in the supraspinatus and infraspinatus of UCP1 reporter mice after undergoing 2 weeks of suprascapular nerve compression versus the contralateral side, but decreased at 2 weeks after release compared with nerve compression (ratio of UCP1 area in the supraspinatus, contralateral: 0.05% ± 0.02%, 95% CI, 0.02%-0.07%; nerve compression: 1.57% ± 0.21%, 95% CI, 1.31%-1.82%; versus contralateral, $p < 0.001$; nerve compression and release: 0.54% ± 0.51%, 95% CI, 0.09%-1.17%; versus contralateral, $p = 0.063$; versus nerve compression, $p = 0.003$; ratio of UCP1 area in the infraspinatus, contralateral: 0.03% ± 0.02%, 95% CI, 0.02%-0.05%; nerve compression: 1.63% ± 0.19%, 95% CI, 1.39%-1.87%; versus contralateral, $p < 0.001$; nerve compression and release: 0.52% ± 0.49%, 95% CI, -0.09% to 1.13%; versus contralateral, $p = 0.056$; versus nerve compression, $p = 0.0016$), suggesting robust beige fat development responding to suprascapular nerve injury (Fig. 8).

Compared with 2-week suprascapular nerve compression in UCP1 (+/+) wild-type mice (collagen area fraction in supraspinatus: 4% ± 1%, 95% CI, 1%-7%; collagen area fraction in infraspinatus: 4% ± 1%, 95% CI, 3%-6%; fat area fraction in supraspinatus: 4% ± 0.27%, 95% CI, 3%-5%; fat area fraction in infraspinatus: 4% ± 1%, 95% CI, 3%-5%), fibrosis and fatty infiltration were reduced after nerve release in UCP1 (+/+) wild-type mice (collagen area fraction in supraspinatus: 2% ± 0.08%, 95% CI, 1.73%-2.13%, $p = 0.044$; collagen area fraction in infraspinatus: 2% ± 1%, 95% CI, 2%-3%, $p = 0.024$; fat area fraction in supraspinatus: 3% ± 0.32%, 95% CI, 2%-4%, $p = 0.0079$; fat area fraction in infraspinatus: 2% ± 1%, 95% CI, 1%-3%, $p = 0.0228$). However, compared with 2 weeks of suprascapular nerve compression in the UCP1 (+/+) wild-type mice, we observed more fibrosis and fatty infiltration in the supraspinatus and infraspinatus of the UCP1-KO mice after 2 weeks of nerve compression (collagen area fraction in supraspinatus: 9% ± 1%, 95% CI, 5%-12%, $p = 0.011$; collagen area fraction in

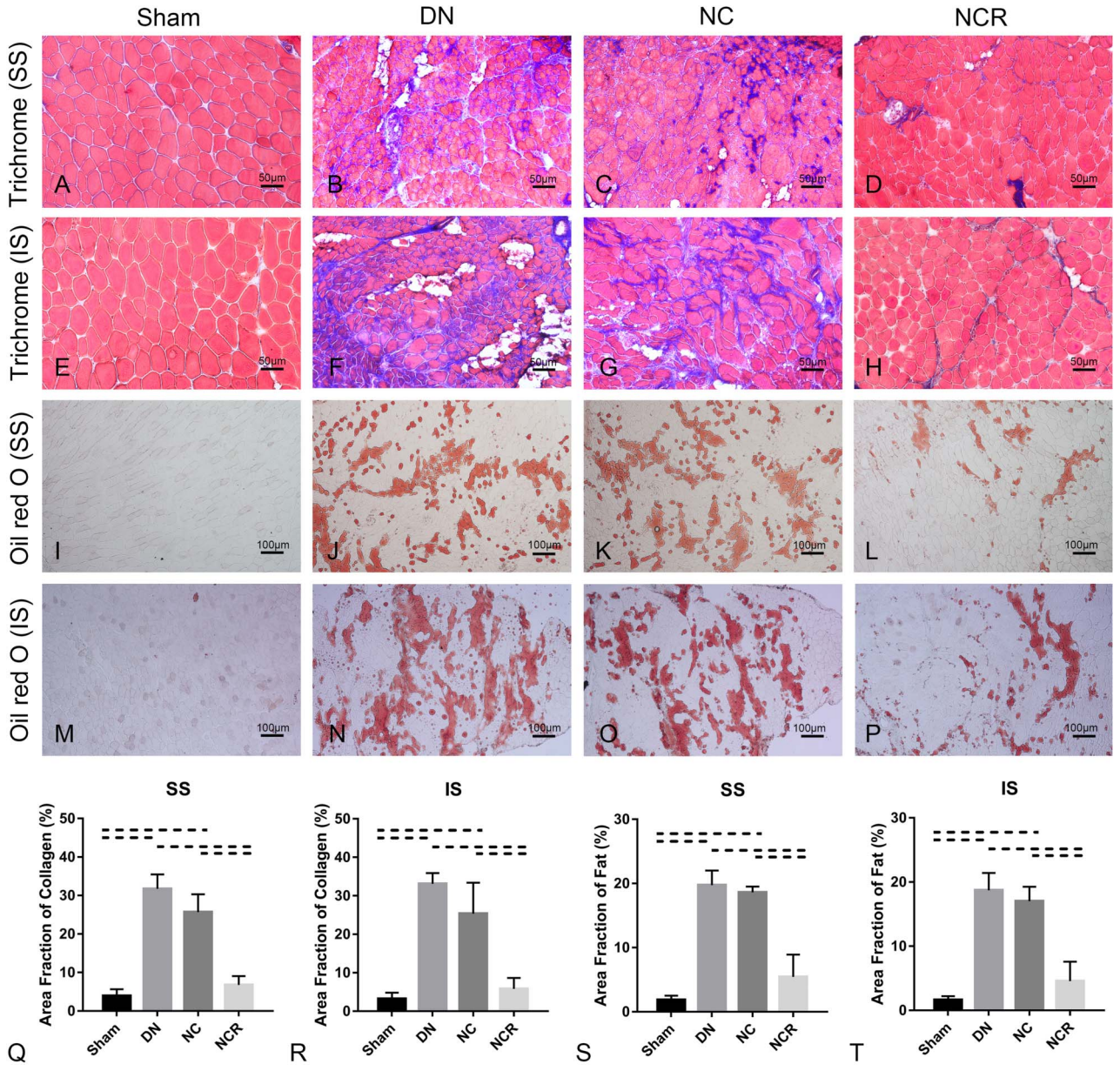

Fig. 5 A-T (**A-H**) Trichrome staining (original magnification, x 200) and (**I-P**) Oil Red O staining (original magnification, x 100) of the supraspinatus and infraspinatus showed fibrosis and fatty infiltration in the supraspinatus and infraspinatus muscles from the denervation group and the nerve compression group, whereas fibrosis and fatty infiltration were decreased in the supraspinatus and infraspinatus muscles from the nerve compression and release group. (**Q-T**) The higher area fraction of collagen and fat was higher in the supraspinatus and infraspinatus in the denervation and the nerve compression groups. Area fraction of collagen (%) = area of collagen staining/entire sample area. Area fraction of fat (%) = area of Oil Red O staining/entire sample area. Solid lines indicate $p < 0.05$ and dashed lines indicate $p < 0.01$. Error bars indicate SD. DN = denervation; NC = nerve compression; NCR = nerve compression and release; SS = supraspinatus; IS = infraspinatus.

infraspinatus: 9% ± 1%, 95% CI, 7%-10%, $p < 0.001$; fat area fraction in supraspinatus: 6% ± 1%, 95% CI, 4%-8%, $p = 0.0106$; fat area fraction in infraspinatus: 6% ± 2%, 95% CI, 4%-8%, $p = 0.032$). Moreover, for UCP1-KO mice, compared with suprascapular nerve compression, we observed no obvious fibrosis and fatty infiltration recovery at 2 weeks after nerve release (collagen area fraction in supraspinatus: 7% ± 1%, 95% CI, 6%-8%, $p = 0.086$; collagen area fraction in infraspinatus: 7% ± 2%, 95% CI, 5%-9%, $p = 0.0916$; fat area fraction in supraspinatus: 5% ± 0.32%, 95% CI, 4%-6%; $p = 0.1095$; fat area fraction in infraspinatus: 5% ± 1%, 95% CI,

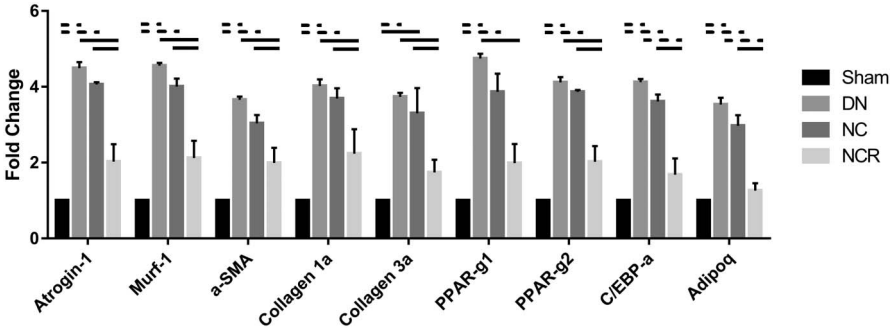

Fig. 6 Atrophy, fibrosis, and fatty infiltration-related gene expression was upregulated 3.5- to 4.5-fold in the denervation group and three- to fourfold in the nerve compression group. No major differences of atrophy, fibrosis, or fatty infiltration-related gene expression were found in the nerve compression and release group when compared with the sham group. Solid lines indicate $p < 0.05$, and dashed lines indicate $p < 0.01$. Error bars indicate SD. DN = denervation; NC = nerve compression; NCR = nerve compression and release.

4%-7%, p = 0.4047) (Fig. 9). This suggests that loss of UCP1 (+) beige fat worsens rotator cuff muscle fatty infiltration after suprascapular nerve compression and prevents fatty infiltration resorption after suprascapular nerve release.

Gait analysis showed that stride length, stance width, and paw area at peak stance of the nerve compression and release group of UCP1-KO mice had reduced shoulder function when compared with the nerve compression and release group of wild-type mice (for wild-type mice, stride length: 2.17 ± 0.37 cm, 95% CI, 1.71-2.63 cm; stance width: 1.24 ± 0.15 cm, 95% CI, 1.05-1.43 cm; paw area at peak stance: 0.20 ± 0.03 cm^2, 95% CI, 0.16-0.24 cm^2; for UCP1-KO mice, stride length: 1.76 ± 0.14 cm, 95% CI, 1.59-1.94 cm, p = 0.0489; stance width: 1.04 ± 0.04 cm, 95% CI, 0.99-1.09 cm, p = 0.024; paw area at peak stance: 0.16 ± 0.01 cm^2, 95% CI, 0.15-0.18 cm^2, p = 0.0399) (Fig. 10).

Discussion

Suprascapular nerve neuropathy may contribute to shoulder dysfunction in patients with large and massive rotator cuff tears. After rotator cuff repair surgery, muscle fatty infiltration may remain and impair shoulder function. In their cadaveric study, Albritton et al. [1] showed that medial retraction of the supraspinatus tendon puts the nerve in tension by changing the angle between the nerve and its first motor branch. Clinical studies also imply a relationship between suprascapular neuropathy and retracted rotator cuff tears with recovery of nerve lesions and improvement of function and symptoms when the tears are repaired [8, 15, 33, 40]. However, the majority of current suprascapular denervation models have been made by nerve transection, which were not reversible. Nerve transection is acute and certainly is the most severe nerve injury, but it is not commonly seen in patients with rotator cuff tears. That being said, denervation

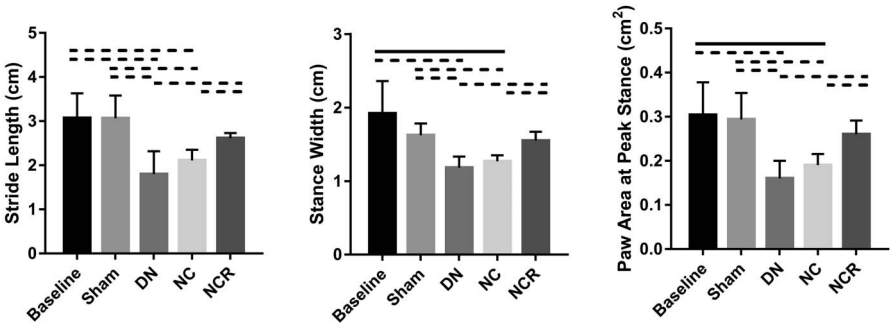

Fig. 7 At 6 weeks postoperatively, gait analysis of the injured forelimb showed that the three parameters in the nerve compression and release group had recovered; however, the three parameters remained at a low level in the denervation group and nerve compression group when compared with the baseline and sham groups. Solid lines indicate $p < 0.05$ and dashed lines indicate $p < 0.01$. Error bars indicate SD. DN = denervation; NC = nerve compression; NCR = nerve compression and release.

Table 2. Correlation of gait analysis and fat area fraction of the nerve compression and release group

	Nerve compression and release group					
	Stride length		Stance width		Paw area at peak stance	
Fat area fraction	r value	p value	r value	p value	r value	p value
Supraspinatus	-0.907	0.033	-0.902	0.036	-0.983	0.003
Infraspinatus	-0.950	0.013	-0.912	0.031	-0.994	0.001

caused by nerve transection may not simulate the fallout from chronic suprascapular nerve injuries as seen in patients with typical rotator cuff tears. In this study, we developed a novel mouse model of reversible suprascapular nerve chronic compression. Compared with an acute suprascapular nerve transection model, this new model has two important improvements. First, suprascapular nerve neuropathy induced in this model is caused by compression rather than transection, which simulates the entrapment of the suprascapular nerve in massive rotator cuff tears. Second, this suprascapular nerve compression model allows recovery of the suprascapular nerve injury by surgically releasing the compression. In this study, we saw reinnervation of rotator cuff muscles after suprascapular nerve compression is released with concomitant muscle recovery. Compared with a nonrecoverable suprascapular nerve transection, this suprascapular nerve compression and release technique used in this new model allows researchers to study the rotator cuff muscle regeneration after suprascapular nerve neuropathy recovery.

This study has several limitations. First, the ligation location of the suprascapular nerve in this model is slightly

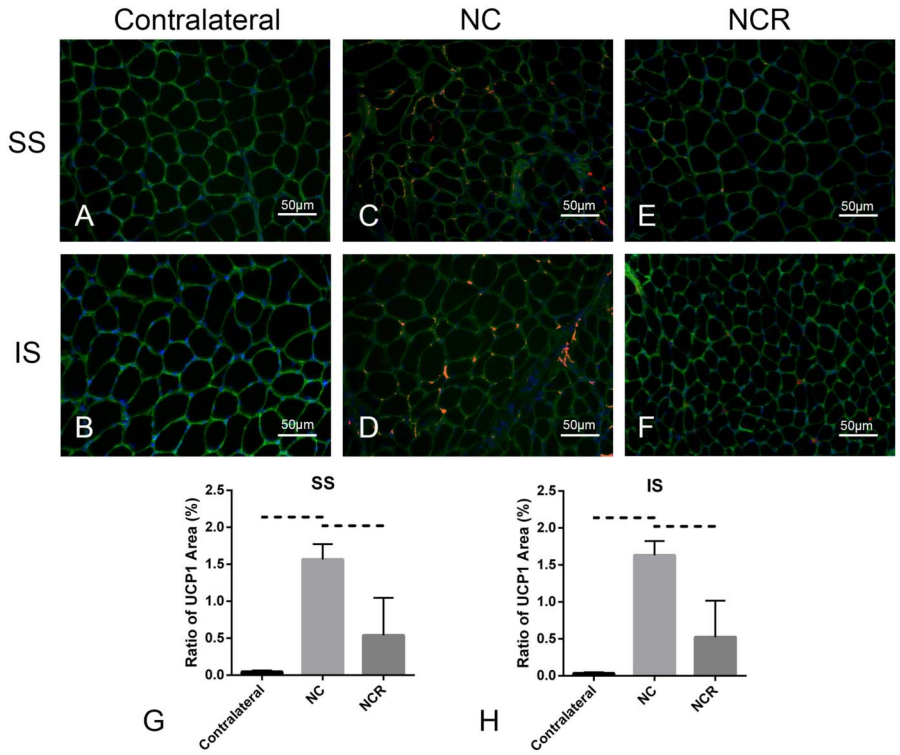

Fig. 8 A-H Immunofluorescent staining (original magnification, x 200) indicated that, compared with the contralateral rotator cuff muscles (**A-B**), UCP1 expression was increased in the supraspinatus and infraspinatus after 2 weeks of suprascapular nerve compression (**C-D**); however, UCP1 expression decreased after compression release for 2 weeks (**E-F**). UCP1 are red, laminin green, and DAPI blue. (**G-H**) Ratio of UCP1 area = the UCP1 area/the entire sample area. Solid lines indicate $p < 0.05$, and dashed lines indicate $p < 0.01$. Error bars indicate SD. DN = denervation; NC = nerve compression; NCR = nerve compression and release.

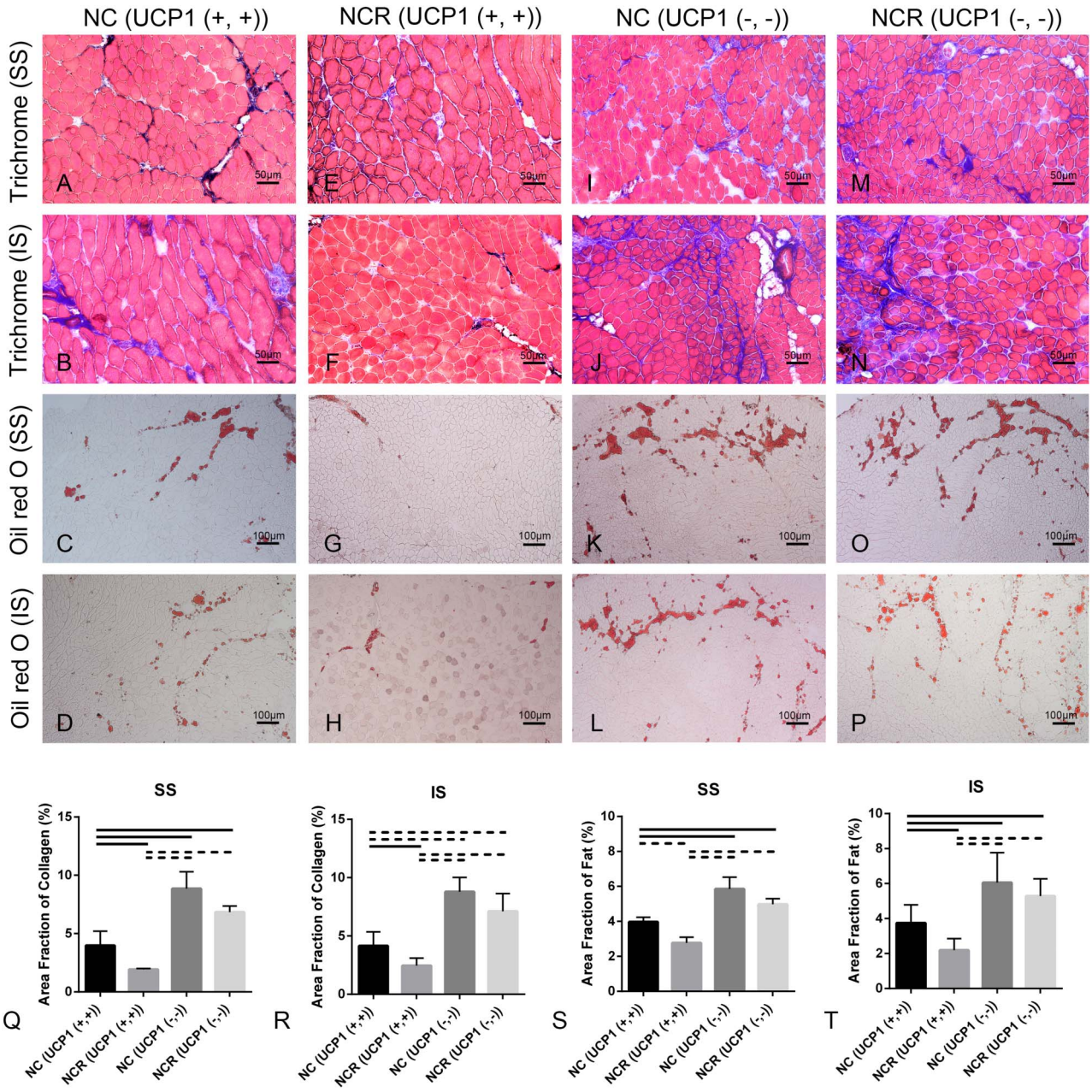

Fig. 9 A-T Trichrome staining (original magnification, x 200) and Oil Red O staining (original magnification, x 100) of the supraspinatus and infraspinatus showed fibrosis and fatty infiltration in the supraspinatus and the infraspinatus of C57BL/N6J mice (UCP1 [+,+]) after 2 weeks of suprascapular nerve compression (**A-D**), which was relieved 2 weeks after release (**E-H**). However, for the UCP1-KO mice, more fibrosis and fatty infiltration in the supraspinatus and infraspinatus was seen after suprascapular nerve compression at 2 weeks (**I-L**), which remained 2 weeks after release (**M-P**). (**Q-T**) Area fraction of collagen (%) = area of collagen staining/entire sample area. Area fraction of fat (%) = area of Oil Red O staining/entire sample area. Solid lines indicate $p < 0.05$, and dashed lines indicate $p < 0.01$. Error bars indicate SD. SS = supraspinatus; IS = infraspinatus; NC = nerve compression; NCR = nerve compression and release.

different from where suprascapular nerve compression happens in massive rotator cuff tears. In the scenario of a large rotator cuff tear, the suprascapular nerve is compressed at the suprascapular notch beneath the supraspinatus muscle. However, in our model, it is impossible to reach the suprascapular notch without injuring the supraspinatus muscle. Thus, we compressed the suprascapular nerve at a higher level, just after it derives from the superior trunk of

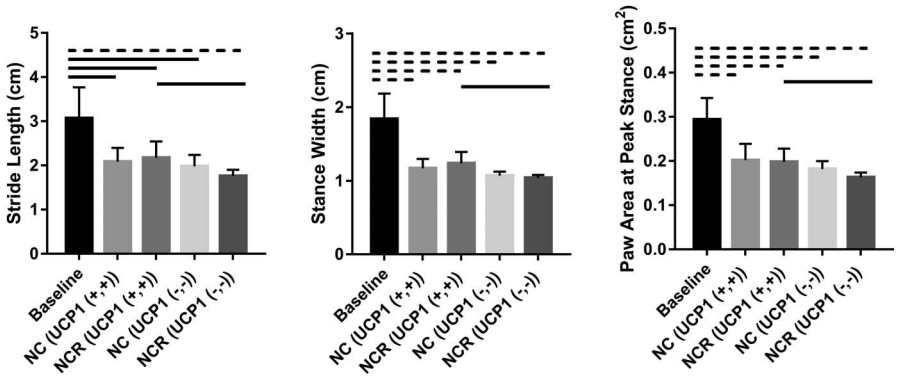

Fig. 10 Gait analysis of the injured forelimb exhibits that stride length, stance width, and paw area at peak stance of the nerve compression and release group of UCP1-KO mice had reduced shoulder function when compared with the nerve compression and release group of wild-type mice. Solid lines indicate $p < 0.05$ and dashed lines indicate $p < 0.01$. Error bars indicate SD. DN = denervation; NC = nerve compression; NCR = nerve compression and release.

the brachial plexus. This allowed us to compress the suprascapular nerve without injuring the supraspinatus or infraspinatus muscles. Second, suprascapular nerve compression is not the only mechanism of suprascapular nerve injury after rotator tears. Retraction of rotator cuff muscle after complete tendon repair may also cause traction injury of the suprascapular nerve. Because both supraspinatus and infraspinatus tendons were intact, suprascapular nerve traction was not simulated in this model. Third, the process of suprascapular nerve compression in this model differs from the typical findings that are seen clinically in the presence of traction. Entrapment of the suprascapular nerve progresses slowly, taking months or years to develop in patients with massive rotator cuff tears. By contrast, in our model, suprascapular nerve compression was immediately and directly induced in our model after the wrapping was placed surgically.

Another limitation was that only selective strains (UCP1 reporter, UCP-1 knockout, and C57B/L6J) of mice were used in this study. C57B/L6 is a commonly used wild-type strain, which are widely used in many orthopedic research studies. In our previous study, we successfully observed severe muscle atrophy and fatty infiltration after massive rotator cuff tendon tears [30]. UCP1 reporter (CD-1 background) and knockout mice (C57B/L6 background) that we used in this study are the only strains available to study UCP1 at this time. In our own literature search, we did not find strain differences in rotator cuff muscle atrophy and fatty infiltration after tendon or nerve injures. However, we will seek to confirm the findings made in this study by evaluating other strains of mice in the future. In addition, we predominantly used young female C57B/L6 mice in this study. It is known that rotator cuff tears are age-related problems with incidence peaking after 40 years of age. The pathophysiology of the rotator cuff muscle after suprascapular nerve compression and release in young individuals may not be identical to those in older ones. Although we did not find sex differences in our pilot study, in future studies, we will recruit mice at different ages and of both sexes. Finally, as a result of the limited transgenic mouse numbers, we only used two time points for UCP1 reporter and knockout mice in this study. Future work with an extended time course will provide more detailed information regarding the involvement of beige fat in muscle fatty infiltration with suprascapular nerve compression and release.

Previous studies have been used botulinum toxin (Botox, Irvine, CA, USA) to study the role of denervation in muscle atrophy and degeneration in the setting of rotator cuff tears. Botulinum toxin selectively binds presynaptically to high-affinity recognition sites on the cholinergic nerve terminals, preventing the release of acetylcholine, which causes a neuromuscular blocking effect on the affected muscle 11. In a rabbit model of chronic rotator cuff tears, Gilotra et al. [14] found an injection of botulinum toxin worsened fatty infiltration in the supraspinatus muscle after tendon transection. Sato et al. [37] reported similar findings in a rat rotator cuff tear model. Although a previous study showed that supraspinatus muscle weight and volume slowly recover from botulinum toxin injection 6 months after tendon repair, muscle histology and function were not evaluated in that study [17]. Thus, it remains unclear if fatty infiltration induced by botulinum toxin in rotator cuff muscles is reversible over time. Compared with botulinum toxin injection, our suprascapular nerve compression and release model has two advantages. First, our model allows precise control for the timing of denervation and reinnervation of the supraspinatus and infraspinatus muscles with surgical

compression and release of the suprascapular nerve. The second advantage, which may be more interesting, is that we observed fast resorption of fatty infiltration in the rotator cuff muscle after suprascapular nerve-releasing compression.

Muscle fatty infiltration is generally considered irreversible, and advanced muscle fatty infiltration is a marker of end-stage rotator cuff disease. Currently, patients with severe muscle fatty infiltration (Goutallier Grade 3 or 4) are not considered good candidates for surgical repair as a result of the high failure rate of tendon repair. Previous preclinical studies with various animal rotator cuff tear models, including our own work with rats [10, 21, 29, 31] and mice [30, 32, 36], also demonstrated irreversible supraspinatus and/or infraspinatus muscle fatty infiltration after tendon and/or nerve injuries. However, in this current study, we observed fat resorption in the supraspinatus and infraspinatus muscles after the release of suprascapular nerve compression. This exciting finding challenges the traditional concept of irreversible rotator cuff muscle fatty infiltration. If suprascapular nerve decompression does reverse muscle fatty infiltration, many patients with Goutallier Grade 3 and 4 muscle fatty infiltration may be qualified for surgical rotator cuff repair through nerve release.

The detailed underlying cellular and molecular mechanisms of muscle fatty infiltration resorption after suprascapular nerve compression remain undefined. However, results from our UCP1 reporter and knockout mice suggest that browning of white fat may be an important mechanism of rotator cuff muscle fatty infiltration resorption. Recently, browning of white fat has become a potential therapeutic intervention to treat obesity and metabolic diseases. Many browning reagents have been discovered and tested. Some of these browning reagents are FDA-approved drugs currently used in the clinic for other indications [7, 41]. For example, PPARγ agonists, thiazolidinediones, are currently used to treat diabetes. A β3-adrenergic receptor agonist, mirabegron, is currently used to treat an overactive bladder. Those white fat browning reagents may serve as future treatments for rotator cuff muscle fatty infiltration.

Regardless of muscle or tendon morphology, one of the most important clinical outcomes for rotator cuff tear repair/rehabilitation is shoulder function. Unlike patients with rotator cuff tears, it is difficult to apply the active joint ROM or other shoulder function testing methods that we use in the clinic to mice. In this study, we adopted a forced downhill running upper limb gait analysis to measure shoulder function in mice. This method has been used for evaluating shoulder function after rotator cuff tears repair 6. In this study, we found that downhill running gait analysis with DigiGait was highly reproducible and consistent among animals within groups. It is also interesting that the gait reduction correlated well with the amount of fat in rotator cuff muscles. These data suggest that forced downhill running upper limb gait analysis is a reliable measurement for shoulder function in mice. It also suggests that rotator cuff muscle fatty infiltration is an important factor for shoulder function.

In summary, we successfully developed a clinically relevant reversible suprascapular nerve compression mouse model. We observed consistent muscle fatty infiltration after nerve compression as well as fatty infiltration resorption after compression release. Future studies will explore how a repair model in combination with nerve compression/release will affect muscle quality and serve as a proxy for studying clinical outcomes as they relate to muscle function. Data from UCP1 reporter and knockout mice suggest that brown/beige fat may play an important role in muscle fatty infiltration resorption after nerve compression release. The mechanism of white fat browning in rotator cuff muscle fatty infiltration and resorption needs to be studied in larger animals and humans to improve clinical outcomes after rotator cuff repair. Given the abundant presence of fibro-/adipogenic progenitor cells after rotator cuff injury, it stands to reason that these cells can be leveraged to transition to beige fat and improve muscle quality after rotator cuff repair. Future studies evaluating pharmacologic treatments to improve "browning" of fibro-/adipogenic progenitor cells will help determine the efficacy of this treatment strategy.

Acknowledgments We thank Dr Shingo Kajimura at the University of California at San Francisco for his kind gifts of UCP1 reporter and UCP1 knockout mice. We also thank Ms Mengyao Liu at the University of California at San Francisco and Ms Kunqi Jiang at the Third Xiangya Hospital of Central South University for their assistance in RT-PCR and data analysis.

References

1. Albritton MJ, Graham RD, Richards RS 2nd, Basamania CJ. An anatomic study of the effects on the suprascapular nerve due to retraction of the supraspinatus muscle after a rotator cuff tear. *J Shoulder Elbow Surg*. 2003;12:497–500.
2. Bachasson D, Singh A, Shah SB, Lane JG, Ward SR. The role of the peripheral and central nervous systems in rotator cuff disease. *J Shoulder Elbow Surg*. 2015;24:1322–1335.
3. Bando Y, Nomura T, Bochimoto H, Murakami K, Tanaka T, Watanabe T, Yoshida S. Abnormal morphology of myelin and axon pathology in murine models of multiple sclerosis. *Neurochem Int*. 2015;81:16–27.
4. Bauder AR, Ferguson TA. Reproducible mouse sciatic nerve crush and subsequent assessment of regeneration by whole mount muscle analysis. *J Vis Exp*. 2012;22: pii: 3606.
5. Beeler S, Ek ET, Gerber C. A comparative analysis of fatty infiltration and muscle atrophy in patients with chronic rotator cuff tears and suprascapular neuropathy. *J Shoulder Elbow Surg*. 2013;22:1537–1546.
6. Bell R, Taub P, Cagle P, Flatow EL, Andarawis-Puri N. Development of a mouse model of supraspinatus tendon insertion site healing. *J Orthop Res.* 2015;33:25–32.

7. Bhatt PS, Dhillo WS, Salem V. Human brown adipose tissue-function and therapeutic potential in metabolic disease. *Curr Opin Pharmacol*. 2017;37:1–9.
8. Costouros JG, Porramatikul M, Lie DT, Warner JJ. Reversal of suprascapular neuropathy following arthroscopic repair of massive supraspinatus and infraspinatus rotator cuff tears. *Arthroscopy*. 2007;23:1152–1161.
9. Coulthard P, Pleuvry BJ, Brewster M, Wilson KL, Macfarlane TV. Gait analysis as an objective measure in a chronic pain model. *J Neurosci Methods*. 2002;116:197–213.
10. Davies MR, Ravishankar B, Laron D, Kim HT, Liu X, Feeley BT. Rat rotator cuff muscle responds differently from hindlimb muscle to a combined tendon-nerve injury. *J Orthop Res.* 2015;33:1046–1053.
11. Dressler D, Saberi FA, Barbosa ER. Botulinum toxin: mechanisms of action. *Arq Neuropsiquiatr*. 2005;63:180–185.
12. Eliasberg CD, Dar A, Jensen AR, Murray IR, Hardy WR, Kowalski TJ, Garagozlo CA, Natsuhara KM, Khan AZ, McBride OJ, Cha PI, Kelley BV, Evseenko D, Feeley BT, McAllister DR, Péault B, Petrigliano FA. Perivascular stem cells diminish muscle atrophy following massive rotator cuff tears in a small animal model. *J Bone Joint Surg Am.* 2017;99:331–341.
13. Eljabu W, Klinger HM, von Knoch M. The natural history of rotator cuff tears: a systematic review. *Arch Orthop Trauma Surg*. 2015;135:1055–1061.
14. Gilotra M, Nguyen T, Christian M, Davis D, Henn RF 3rd, Hasan SA. Botulinum toxin is detrimental to repair of a chronic rotator cuff tear in a rabbit model. *J Orthop Res.* 2015;33:1152–1157.
15. Greiner A, Golser K, Wambacher M, Kralinger F, Sperner G. The course of the suprascapular nerve in the supraspinatus fossa and its vulnerability in muscle advancement. *J Shoulder Elbow Surg*. 2003;12:256–259.
16. Hast MW, Zuskov A, Soslowsky LJ. The role of animal models in tendon research. *Bone Joint Res.* 2014;3:193–202.
17. Hettrich CM, Rodeo SA, Hannafin JA, Ehteshami J, Shubin Stein BE. The effect of muscle paralysis using Botox on the healing of tendon to bone in a rat model. *J Shoulder Elbow Surg*. 2011;20:688–697.
18. Jeremic N, Chaturvedi P, Tyagi SC. Browning of white fat: novel insight into factors, mechanisms, and therapeutics. *J Cell Physiol*. 2017;232:61–68.
19. Jin J, Limburg S, Joshi SK, Landman R, Park M, Zhang Q, Kim HT, Kuo AC. Peripheral nerve repair in rats using composite hydrogel-filled aligned nanofiber conduits with incorporated nerve growth factor. *Tissue Eng Part A*. 2013;19:2138–2146.
20. Joshi SK, Kim HT, Feeley BT, Liu X. Differential ubiquitin-proteasome and autophagy signaling following rotator cuff tears and suprascapular nerve injury. *J Orthop Res.* 2014;32:138–144.
21. Joshi SK, Liu X, Samagh SP, Lovett DH, Bodine SC, Kim HT, Feeley BT. mTOR regulates fatty infiltration through SREBP-1 and PPARgamma after a combined massive rotator cuff tear and suprascapular nerve injury in rats. *J Orthop Res.* 2013;31:724–730.
22. Kajimura S, Saito M. A new era in brown adipose tissue biology: molecular control of brown fat development and energy homeostasis. *Annu Rev Physiol*. 2014;76:225–249.
23. Kajimura S, Spiegelman BM, Seale P. Brown and beige fat: physiological roles beyond heat generation. *Cell Metab*. 2015;22:546–559.
24. Kim SH, Plutzky J. Brown fat and browning for the treatment of obesity and related metabolic disorders. *Diabetes Metab J*. 2016;40:12–21.
25. Kinds MB, Bartels LW, Marijnissen AC, Vincken KL, Viergever MA, Lafeber FP, de Jong HW. Feasibility of bone density evaluation using plain digital radiography. *Osteoarthritis Cartilage*. 2011;19:1343–1348.
26. Krieger JR, Tellier LE, Ollukaren MT, Temenoff JS, Botchwey EA. Quantitative analysis of immune cell subset infiltration of supraspinatus muscle after severe rotator cuff injury. *Regen Eng Transl Med*. 2017;3:82–93.
27. Leclere LE, Shi LL, Lin A, Yannopoulos P, Higgins LD, Warner JJ. Complete fatty infiltration of intact rotator cuffs caused by suprascapular neuropathy. *Arthroscopy*. 2014;30:639–644.
28. Lin JZ, Farmer SR. Morphogenetics in brown, beige and white fat development. *Adipocyte*. 2016;5:130–135.
29. Liu X, Joshi SK, Samagh SP, Dang YX, Laron D, Lovett DH, Bodine SC, Kim HT, Feeley BT. Evaluation of Akt/mTOR activity in muscle atrophy after rotator cuff tears in a rat model. *J Orthop Res.* 2012;30:1440–1446.
30. Liu X, Laron D, Natsuhara K, Manzano G, Kim HT, Feeley BT. A mouse model of massive rotator cuff tears. *J Bone Joint Surg Am.* 2012;94:e41.
31. Liu X, Manzano G, Kim HT, Feeley BT. A rat model of massive rotator cuff tears. *J Orthop Res.* 2011;29:588–595.
32. Liu X, Ning AY, Chang NC, Kim H, Nissenson R, Wang L, Feeley BT. Investigating the cellular origin of rotator cuff muscle fatty infiltration and fibrosis after injury. *Muscles Ligaments Tendons J*. 2016;6:6–15.
33. Mallon WJ, Wilson RJ, Basamania CJ. The association of suprascapular neuropathy with massive rotator cuff tears: a preliminary report. *J Shoulder Elbow Surg.* 2006;15:395–398.
34. New Zealand Animal Welfare Act 1999. Available at: http://www.legislation.govt.nz/act/public/1999/0142/latest/DLM49664.html. Accessed June 16, 2015.
35. Sachinis NP, Boutsiadis A, Papagiannopoulos S, Ditsios K, Christodoulou A, Papadopoulos P. Suprascapular neuropathy in the setting of rotator cuff tears: study protocol for a double-blinded randomized controlled trial. *Trials*. 2016;17:554.
36. Samagh SP, Kramer EJ, Melkus G, Laron D, Bodendorfer BM, Natsuhara K, Kim HT, Liu X, Feeley BT. MRI quantification of fatty infiltration and muscle atrophy in a mouse model of rotator cuff tears. *J Orthop Res.* 2013;31:421–426.
37. Sato EJ, Killian ML, Choi AJ, Lin E, Esparza MC, Galatz LM, Thomopoulos S, Ward SR. Skeletal muscle fibrosis and stiffness increase after rotator cuff tendon injury and neuromuscular compromise in a rat model. *J Orthop Res.* 2014;32:1111–1116.
38. Shirasawa H, Matsumura N, Shimoda M, Oki S, Yoda M, Tohmonda T, Kanai Y, Matsumoto M, Nakamura M, Horiuchi K. Inhibition of PDGFR signaling prevents muscular fatty infiltration after rotator cuff tear in mice. *Sci Rep*. 2017;7:41552.
39. Sidossis L, Kajimura S. Brown and beige fat in humans: thermogenic adipocytes that control energy and glucose homeostasis. *J Clin Invest*. 2015;125:478–486.
40. Vad VB, Southern D, Warren RF, Altchek DW, Dines D. Prevalence of peripheral neurologic injuries in rotator cuff tears with atrophy. *J Shoulder Elbow Surg*. 2003;12:333–336.
41. Wankhade UD, Shen M, Yadav H, Thakali KM. Novel browning agents, mechanisms, and therapeutic potentials of brown adipose tissue. *Biomed Res Int*. 2016;2016:2365609.